The FEBS Journal

FEBS PRESS science publishing by scientists

Functional consequences of lysine acetylation of phosphofructokinase isozymes

Xinyu Li[1], Nour Fatema[1], Qinglei Gan[2] and Chenguang Fan[1,2]

1 Cell and Molecular Biology Program, University of Arkansas, Fayetteville, AR, USA
2 Department of Chemistry and Biochemistry, University of Arkansas, Fayetteville, AR, USA

Keywords
deacetylase; genetic code expansion; glycolysis; lysine acetylation; phosphofructokinase

Correspondence
C. Fan, University of Arkansas, CHEM 119, 345 N Campus Walk, Fayetteville, AR 72701, USA
Tel: +1 479 575 4653
E-mail: cf021@uark.edu

(Received 1 October 2024, revised 6 December 2024, accepted 31 January 2025)

doi:10.1111/febs.70014

Phosphofructokinase (Pfk) catalyzes the phosphorylation of fructose 6-phosphate and is a key regulatory point in the glycolysis pathway. Multiple lysine residues in both Pfk isozymes, PfkA and PfkB, have been identified to be acetylated in *Escherichia coli* by proteomic studies, but no studies have been implemented to further characterize these acetylation events. To investigate the role of Pfk acetylation, the genetic code expansion strategy was used to generate homogeneously acetylated Pfk variants at target lysine sites that have been reported to be acetylated in nature. We found that acetylation of K309 of PfkA and K27 of PfkB decreased PfK enzyme activities significantly. We further investigated the deacetylation and acetylation processes of Pfk isozymes biochemically and genetically. Acetyl phosphate-mediated non-enzymatic acetylation could be the major mechanism of Pfk isozyme acetylation in *E. coli*, whereas NAD-dependent protein deacylase CobB can remove most of the acetylated lysine residues but not K309 of PfkA and K27 of PfkB, which affect enzyme activities. Because of the important role of Pfk in cellular metabolism, the results of the present study are expected to facilitate studies in the fields of metabolic engineering and research.

Introduction

Phosphofructokinase (Pfk) (EC2.7.1.11) catalyzes the phosphorylation of the C1 carbon of fructose 6-phosphate (F-6-P) to generate fructose 1,6-bisphosphate (F-1,6-BP) in the glycolysis pathway. It is one of the key regulatory points of glycolysis [1]. In *Escherichia coli*, there are two Pfk isozymes, PfkA and PfkB. These two Pfk isozymes share a low sequence identify (< 15%) (Fig. S1) and belong to different homology families [2]. PfkA is a member of the ATP- or pyrophosphate-dependent PFKA family found in eukaryotes and bacteria. Most eukaryotic ATP PFKs have evolved from the bacterial PFK by gene duplication and fusion events [3]. PfkB belongs to the ribokinase family of sugar kinases, which are distinct in sequence and structure from the PFKA family [4,5]. These two Pfk isozymes play different roles in glycolysis. PfkA contributes most of the phosphofructokinase activity in *E. coli* cells. The Δ*pfkA* strain can still grow with glucose relying on the presence of *pfkB*, whereas the double mutant Δ*pfkA* Δ*pfkB* cannot grow in the glucose medium [6]. Besides the role in glycolysis, PfkA can also catalyze the phosphorylation of sedoheptulose 7-phosphate in the sedoheptulose bisphosphate bypass [7], whereas PfkB can add another phosphate to tagatose 6-phosphate as part of the galactitol degradation pathway [8]. Both Pfk isozymes can be allosterically inhibited by ATP [9,10], thus avoiding a futile cycle of ATP

Abbreviations
AcCoA, acetyl-CoA; AcK, acetylated lysine; AcP, acetyl phosphate; CD, circular dichroism; F-1,6-BP, fructose 1,6-bisphosphate; F-6-P, fructose 6-phosphate; LB, Luria–Bertani; LC-MS/MS, liquid chromatography-tandem mass spectrometry; KQ, lysine to glutamine substitution; KR, lysine to arginine substitution; PDB, Protein Data Bank; PEP, phosphoenolpyruvate; Pfk, phosphofructokinase; PVDF, poly (vinylidene difluoride); WT, wild-type.

hydrolysis under gluconeogenesis conditions [11]. However, only PfkA shows cooperative kinetics with F-6-P, inhibition by phosphoenolpyruvate (PEP), and activation by ADP or GDP [8,12]. As a result of the key role in the glycolysis pathway, Pfk has been a favorable target in metabolic engineering. Pfk-deficient strains have been used to increase NADPH generation by directing F-6-P oxidation through the pentose phosphate pathway [13]. Similar strategies have been adopted to increase production of various compounds such as L-threonine [14], D-glucose [15], mevalonate [16], *N*-acetylglucosamine [17], D-mannose [18] and 5-methyltetrahydrofolate [19]. Thus, it is important to investigate the regulation of Pfk isozymes in *E. coli* cells.

Lysine acetylation is not only unique for eukaryotic, but also exists widely in bacteria, as supported by a series of proteomic studies [20,21]. Notably, metabolic enzymes are favorable targets for lysine acetylation, showing the potential role of lysine acetylation in controlling cellular metabolism in bacteria [22–24]. The acetylome database in the Compendium of Protein Lysine Modifications shows that both Pfk isozymes in *E. coli* have multiple acetylated lysine residues existing in nature [25]. However, no further studies have been implemented to characterize those acetylated Pfk variants, and whether lysine acetylation regulates Pfk function remains largely unanswered.

Glutamine has been commonly used as the mimic of acetylated lysine residue to characterize the function of acetylation in target proteins [26–28]. Unfortunately, the size difference between authentic acetylated lysine (AcK) and glutamine could mislead the results from the glutamine-substitution approach. Indeed, our studies on acetylation of isocitrate dehydrogenase and glucokinase have demonstrated such discrepancy [29,30]. To generate target proteins with authentic AcK at specific sites, several approaches have been developed. Among them, genetic code expansion is a facile method to produce homogeneously acetylated proteins with authentic AcK at target lysine sites [31]. This strategy introduces an orthogonal pair of a pyrrolysyl-tRNA synthetase variant evolved to recognize AcK and a $tRNA^{Pyl}$ harboring a stop anticodon into host cells and uses the host translation machinery to decode an introduced stop codon (replacing the corresponding lysine codon in the gene of the target protein) as AcK, thus generating a site-specifically acetylated protein without laborious and harsh chemical reactions. In the present study, we used this approach to study the impact of lysine acetylation on Pfk isozyme activity site-specifically. Furthermore, we applied both biochemical and genetic approaches to explore the processes of acetylation and deacetylation of Pfk isozymes. Because the essential role of Pfk isozymes in cellular metabolism, the results of the present study are expected to contribute to both bacterial metabolism studies and metabolic engineering.

Results

Production of site-specifically acetylated *E. coli* Pfk isozyme variants

There are multiple acetylation sites in both *E. coli* Pfk isozymes identified by a series of proteomic studies. To identify the key sites regulating Pfk function, we aimed to determine the impact of lysine acetylation on Pfk isozymes site-by-site. However, the currently reported lysine acetylation sites by different proteomic studies do not converge well, possibly because these studies applied different enrichment approaches and identification methods for acetylated peptides and worked on distinct *E. coli* strains [32–36]. To generate unbiased results, we chose all the nine reported lysine acetylation sites in PfKA or PfkB to date, including K91, K237, K305, K309 of PfkA and K27, K148, K158, K189, K302 of PfkB.

Glutamine could not always be a sufficient mimic for authentic acetylated lysine residue, and so we applied the genetic code expansion strategy to produce Pfk isozyme variants with homogeneously acetylated lysine residues at each target site by an optimized AcK incorporation system [37]. We utilized *E. coli* BL21 (DE3) cells as host cells to express PfK variants recombinantly because this strain has a relatively low background level of global lysine acetylation, thus minimizing the interference from background acetylation [32]. To apply the AcK incorporation system, a TAG stop codon was introduced into the *pfkA or pfkB* gene to replace the corresponding lysine codon by site-directed mutagenesis and confirmed by DNA sequencing individually. To remove truncated proteins by early termination at introduced stop codons, we added a His6 affinity tag to the C-termini of Pfk variants for easy separation because only full-length proteins retain the affinity tag. SDS/PAGE gels showed that all Pfk variants had good purify for further experiments. Western blotting demonstrated that all acetylated Pfk variants were recognized by the AcK antibody, whereas purified wild-type (WT) PfkA and PfkB have no detectable lysine acetylation (Fig. 1; see also Figs S2 and S3). To further confirm those Pfk variants have lysine acetylation at correct sites, liquid chromatography-tandem mass spectrometry (LC-MS/MS) analyses have been implemented (Figs S4–S12).

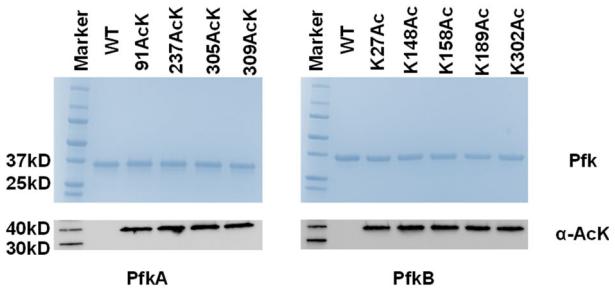

Fig. 1. Production of site-specifically acetylated *Escherichia coli* Pfk isozyme variants. SDS/PAGE and western blotting analyses of purified PfkA and PfkB and their site-specifically acetylated variants. The same amounts of purified proteins were loaded on each lane. WT, wild type; α-AcK, the acetyllysine antibody. The full images of western blotting are provided in Figs S2 and S3. The images are representative of three replicates.

The deacetylation process of Pfk isozymes

Deacetylase catalyzes the reverse reaction of acetylation, converting AcK back to free lysine residue. It is significant to determine the substate specificities of deacetylases not only for obtaining fundamental knowledge of lysine acetylation, but also for guiding medical applications because of the association of lysine acetylation with many diseases such as leukemia and neurodegenerative diseases [38,39]. One practical application of genetic code expansion in acetylation studies is to determine the substate specificity of deacetylases. Using site-specifically acetylated proteins as substrates, we can determine whether the target protein is the substrate for the selected deacetylase. Furthermore, this approach can also demonstrate the specificity of the selected deacetylase to the level of specific lysine residues.

Although there are several proposed deacetylases in *E. coli*, CobB is the only well-characterized one to date [40,41]. Thus, we first determined the specificity of CobB for both PfkA and PfkB *in vitro*. Each purified acetylated PfkA or PfkB variant generated by the genetic code expansion strategy was incubated with CobB and its cofactor NAD^+ for 1 h and then tested by western blotting (Fig. 2A; see also Fig. S13). Most acetylated Pfk isozyme variants had no detectable acetylation after CobB-treatment. Two acetylation sites, K309 of PfkA and K27 of PfkB, were resistant to CobB *in vitro*. As shown in Fig. 2B, these two CobB-resistant lysine sites face to the interior of enzymes, and so CobB could not approach them for deacetylation because of steric hindrance.

Next, we tested CobB-dependent deacetylation of PfkA and PfkB *in vivo*. To avoid possible interferences between isozymes, native PfkA was purified from Δ*pfkB* and Δ*cobB* Δ*pfkB* strains of BW25113 cells, whereas native PfkB was purified from Δ*pfkA* and Δ*cobB* Δ*pfkA* strains of BW25113 cells. Western blotting was performed to determine the acetylation levels of Pfk isozymes (Fig. 2C; see also Fig. S14). Clearly, *cobB*-inactivation increased acetylation levels of both PfkA and PfkB *in vivo*, consistent with our *in vitro* results indicating that CobB can deacetylate most of acetylation sites in both Pfk isozymes.

The acetylation process of Pfk isozymes

Different from the deacetylation process, which is commonly catalyzed by enzymes, the acetylation process can be mediated by enzymes or chemicals alone such as acetyl-CoA (AcCoA) and acetyl phosphate (AcP) [20,42]. We first tested the enzyme-dependent acetylation of Pfk isozymes. To date, YfiQ is the only well-characterized protein acetyltransferase in *E. coli* [43]. Native PfkA was purified from Δ*pfkB* and Δ*yfiQ* Δ*pfkB* strains of BW25113 cells, whereas native PfkB was purified from Δ*pfkA* and Δ*yfiQ* Δ*pfkA* strains of BW25113 cells to avoid possible interferences between isozymes. The acetylation levels of native Pfk isozymes were determined by western blotting (Fig. 3A; see also Fig. S15). Inactivation of *yifQ* did not decrease the acetylation levels of both Pfk isozymes significantly. To exclude the possibility that CobB in cells could remove the acetylation of Pfk isozymes catalyzed by YfiQ, we further determined the acetylation levels of Pfk isozymes from corresponding Δ*pfk* Δ*yfiQ* Δ*cobB* strains (Fig. 3A). Their acetylation levels were similar to those from corresponding Δ*pfk* Δ*cobB* strains, suggesting that YfiQ is not the major acetyltransferase for Pfk isozymes *in vivo*. In addition, we incubated purified WT Pfk isozymes expressed from BL21(DE3) cells, which had no detectable acetylation (Fig. 1), with purified YfiQ and its cofactor AcCoA *in vitro*. Western blotting showed that YfiQ cannot acetylate both Pfk isozymes *in vitro*, supporting the *in vivo* results (Fig. 3B; see also Fig. S16). One recent proteomic study has identified four new protein acetyltransferases in *E. coli*, including RimI, YiaC, YjaB and PhnO [44]. However, the data from this study showed that overexpressing each of those four acetyltransferases did not increase the acetylation levels of both Pfk isozymes, indicating that enzyme-dependent acetylation may not be the major mechanism of Pfk isozyme acetylation.

Next, we investigated non-enzymatic acetylation of Pfk isozymes. In the *in vitro* YfiQ-dependent acetylation assay above, the concentration of AcCoA in the assay was 0.2 mM, corresponding to the intracellular

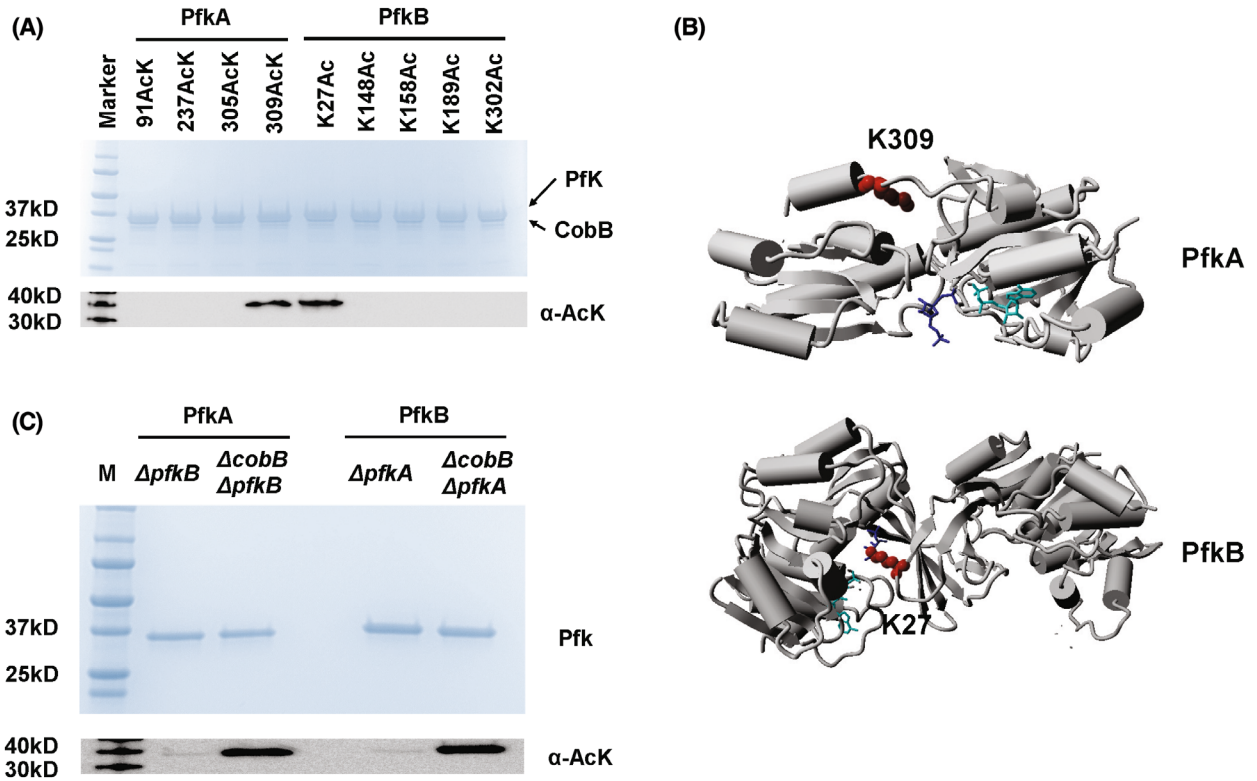

Fig. 2. Deacetylation of *Escherichia coli* Pfk isozymes by CobB. (A) SDS/PAGE and western blotting analyses of site-specifically acetylated Pfk isozymes variants after incubation with purified CobB *in vitro*. (B) Mapping of two CobB-resistant sites onto the crystal structures of *E. coli* PfkA monomer [Protein Data Bank (PDB) ID: 1PFK] and PfkB dimer (PDB ID: 3UQD). Two acetylation sites are indicated in red. Fructose 1,6-bisphosphate (F-1,6-BP) in PfkA and fructose 6-phosphate (F-6-P) in PfkB are indicated in blue, whereas ADP in PfkA and ATP in PfkB are indicated in cyan. The structure was demonstrated using YASARA (https://www.yasara.org). (C) SDS/PAGE and western blotting analyses of native Pfk isozymes purified from corresponding Δ*pfk* and Δ*cobB* Δ*pfk* of BW25113 cells grown in Luria–Bertani (LB) media. M, marker; α-AcK, the acetyllysine antibody. The full images of the western blotting are provided in Figs S13 and S14. The images are representative of three replicates.

concentration of AcCoA in *E. coli* cells [45]. Western blotting showed that both Pfk isozymes had no detectable acetylation after incubation with 0.2 mM AcCoA alone (Fig. 3B, lanes 2 and 6). Then, we tested AcP-mediated acetylation, which is suggested to be the major acetylation mechanism in *E. coli* [32]. Purified WT Pfk isozymes expressed from BL21(DE3) cells, which had no detectable acetylation (Fig. 1), were incubated with 1 mM AcP, corresponding to intracellular AcP concentration in *E. coli* cells [46]. Western blotting was implemented to determine the acetylation levels of AcP-treated Pfk isozymes with different incubation time. One millimolar AcP alone could acetylate both Pfk isozymes in a time-dependent manner (Fig. 4A; see also Fig. S17). We further performed LC-MS/MS analyses to identify acetylation sites in Pfk isozymes treated with 1 mM AcP *in vitro*. All of the nine reported acetylation sites were found by MS analyses. Similar to our previous studies [47–49], we also identified five non-reported acetylation sites, including K4, K212, K317 of PfkA and K207, K217 of PfkB (Figs S18–S22) and their roles require further characterization.

Thus, we further tested AcP-mediated acetylation of Pfk isozymes *in vivo*. The AcP metabolism in *E. coli* is mostly associated with two enzymes. AckA, acetate kinase, catalyzes the conversion between acetate and AcP, whereas Pta, phosphate acetyltransferase, catalyzes the conversion between AcCoA and AcP. In non-acetate growth media such as glucose media, inactivation of *ackA* will accumulate AcP, whereas inactivation of *pta* will limit the amount of AcP in *E. coli* cells. Then, native PfkA was purified from Δ*pfkB*, Δ*pta* Δ*pfkB* and Δ*ackA* Δ*pfkB* strains of BW25113 cells, whereas native PfkB was purified from Δ*pfkA*, Δ*pta* Δ*pfkA* and Δ*ackA* Δ*pfkA* stains of BW25113 cells to avoid possible interferences between isozymes. All strains were growth in 0.2% glucose media. Western

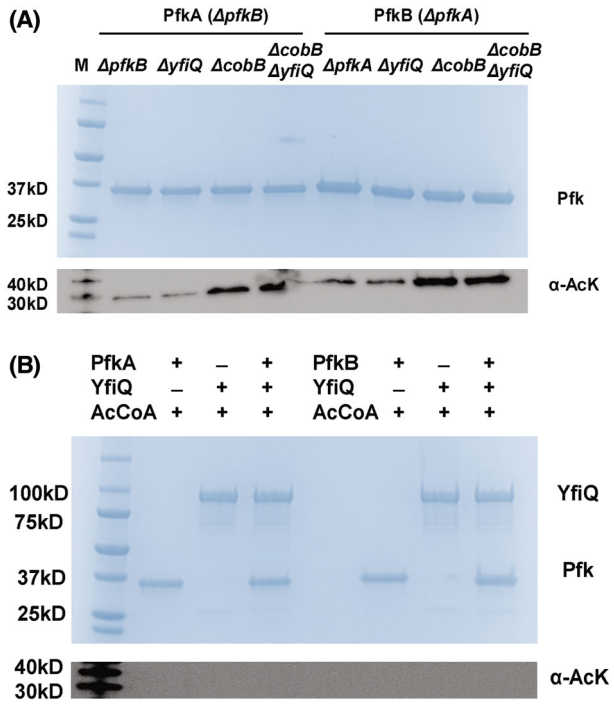

Fig. 3. YfiQ-dependent acetylation of Pfk isozymes. (A) SDS/PAGE and western blotting analyses of purified native PfkA and PfkB from corresponding Δ*pfk*, Δ*yfiQ*, Δ*cobB* or Δ*yfiQ* Δ*cobB* strains of BW25113 cells grown in LB media. (B) SDS/PAGE and western blotting analyses of purified recombinantly expressed Pfk isozymes from BL21(DE3) cells incubated with purified YfiQ and 0.2 mM acetyl-CoA (AcCoA) for 1 h. M, marker; α-AcK, the acetyllysine antibody. The full images of western blotting are provided in Figs S15 and S16. The images are representative of three replicates.

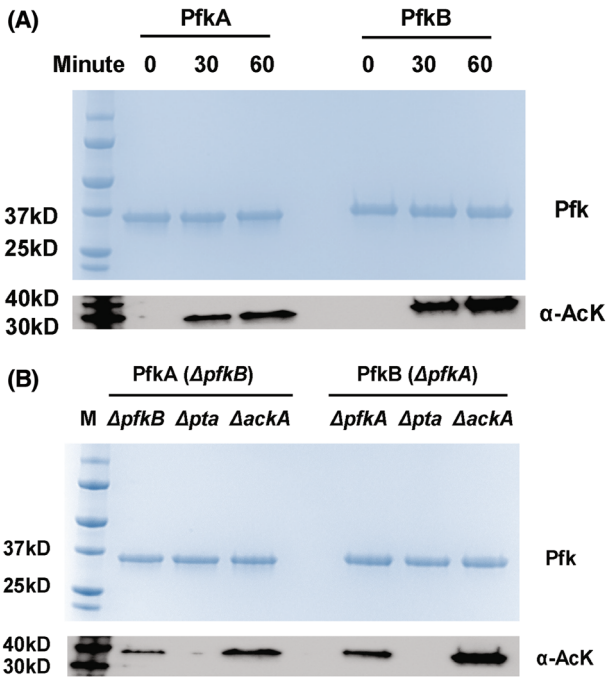

Fig. 4. Acetyl phosphate (AcP)-mediated acetylation of Pfk isozymes. (A) SDS/PAGE and western blotting analyses of purified Pfk isozymes from BL21(DE3) cells treated with 1 mM AcP *in vitro* at 0, 30 and 60 min. (B) SDS/PAGE and western blotting analyses of native PfkA and PfkB purified from corresponding Δ*pfk*, Δ*pta* or Δ*ack* of BW25113 cells grown in 0.2% glucose media. M, marker; α-AcK, the acetyllysine antibody. The full images of western blotting are provided in Figs S17 and S23. The images are representative of three replicates.

blotting was performed to determine the acetylation levels of purified Pfk isozymes (Fig. 4B; see also Fig. S23). Both native Pfk isozymes purified from cells grown in glucose media (Fig. 4B, lanes 2 and 6) had higher acetylation levels than those purified from cells grown in Luria–Bertani (LB) media (Fig. 3A, lanes 2 and 6), consisting with previous studies which showed that glucose induced a higher acetylation level globally in *E. coli* [32,34]. The non-detectable acetylation of Pfk isozymes in *Δpta* strains and enhanced acetylation of Pfk isozymes in Δ*ackA* strains supported the *in vitro* AcP-mediated acetylation results and suggested that non-enzymatic acetylation by AcP could be the major acetylation mechanism for Pfk isozymes.

The site-specific effects of lysine acetylation on Pfk isozyme activities

We fused the His6-tag to the C-termini of Pfk isozymes to facilitate purification. However, a previous study showed that the C-terminus of PfkB is essential for both regulatory properties and quaternary structures [50]. To avoid potential interferences, we first examined the saturation curves for both MgATP and F-6-P with purified His6-tagged and non-tagged PfkB (Fig. S24). The saturation curves of His6-tagged PfkB were similar to those of non-tagged PfkB, indicating that the C-terminal His6-tag has limited effects on PfkB activity.

Then, we performed enzyme assays to measure activities of purified WT and site-specifically acetylated Pfk isozyme variants. Both substrates F-6-P and MgATP were fixed at 1 mM (i.e. the concentrations corresponding to the maximum activity). Most Pfk variants had similar activities to WT PfkA or PfkB (Fig. 5A). There were two acetylated variants, PfkA-309AcK and PfkB-27AcK, which had significantly decreased activities compared with corresponding WT enzymes. The PfkA-309AcK variant retained approximately 70% of the WT PfkA activity, whereas acetylation of K27 in PfkB decreased the PfkB activity by

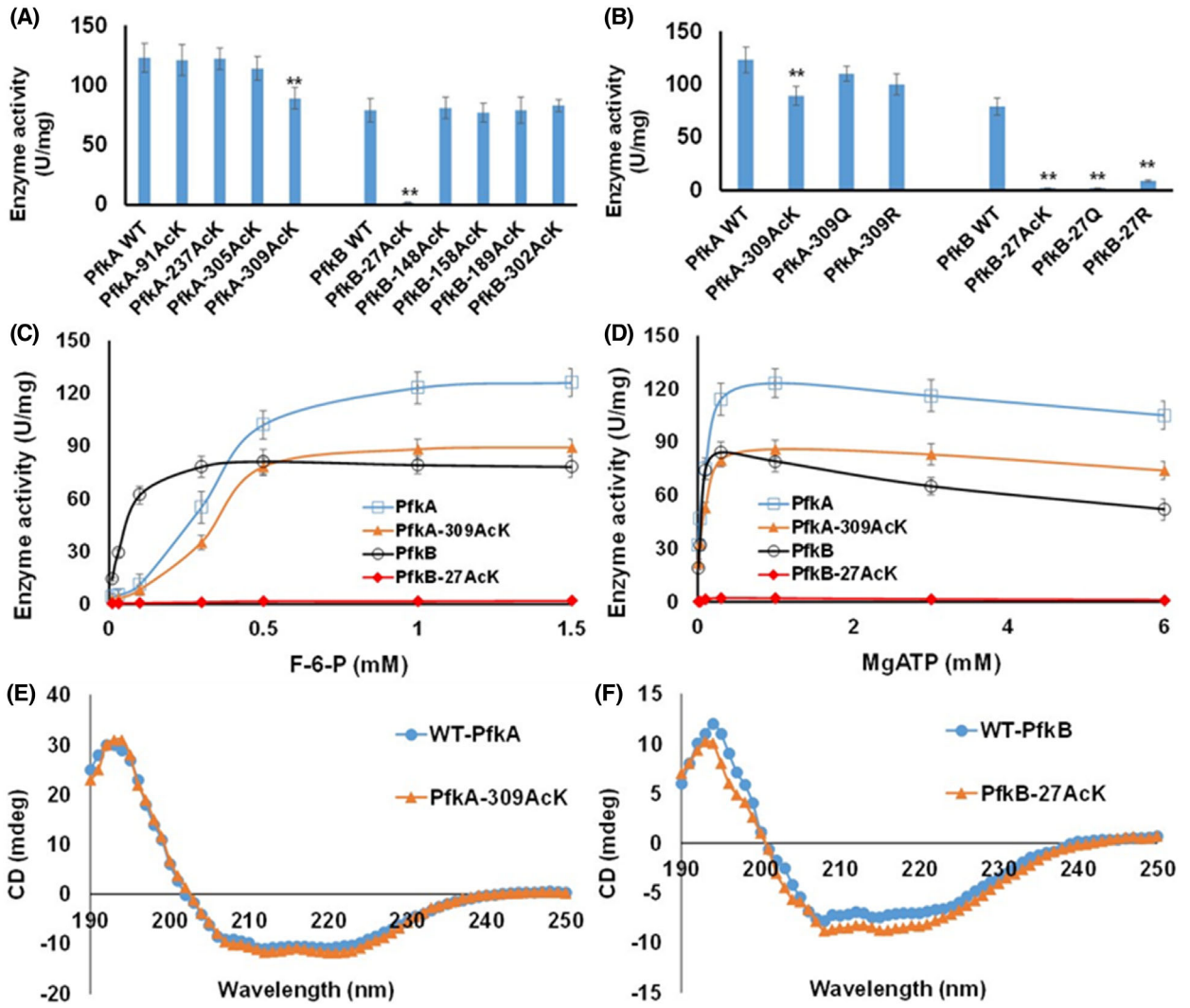

Fig. 5. Characterization of Pfk isozyme variants. (A) Enzyme activities of *Escherichia coli* Pfk isozymes and their site-specifically acetylated variants. (B) Enzyme activities of *E. coli* Pfk isozymes and their KQ- and KR-substitution variants. Two-tailed *P* values were determined via a *t*-test, and the significance level is 0.05. $^{**}P < 0.001$. For enzyme activities, 1 unit (U) is defined as 1 μmol product generation per minute. Both fructose 6-phosphate (F-6-P) and MgATP were fixed at 1 mM. The mean ± SD values were calculated based on three replicates. (C) The Pfk activity as a function of F-6-P concentration. MgATP was fixed at 1 mM. (D) The Pfk activity as a function of MgATP concentration. F-6-P was fixed at 1 mM F-6-P. The mean ± SD values were calculated based on three replicates. The activity without substrates was used as the baseline (zero) for calculation. (E) The circular dichroism (CD) spectra of WT PfkA and PfkA-309AcK. (F) The CD spectra of WT PfkB and PfkB-27AcK. Scanning was performed from 190 to 250 nm with a speed of 60 nm·min^{-1} five times for each sample and the average was plotted.

almost 100-fold. As shown in Fig. 2B, K27 is located at the active size and important for the catalytic process.

Classic acetylation studies use glutamine as the mimic of acetylated lysine and arginine as the mimic of non-acetylated lysine, so we also generated glutamine (KQ)- or arginine (KR)-substitution variants for K309 of PfkA and K27 of PfkB. Enzyme assays were implemented to measure their activities (Fig. 5B). Neither KQ- nor KR-mutation at K309 of PfkA affected PfkA activity significantly. It is noteworthy that glutamine is not a sufficient substitution for authentic acetylation for this lysine site. For the other lysine site K27 of PfkB, both KQ- and KR-mutations caused significant decreases in its activity. The KQ-mutation had a similar effect to authentic acetylation, whereas the

KR-mutation restored approximately 15% of the PfkB activity.

We further examined the saturation curves of WT PfkA and PfkB as well as PfkA-309AcK and PfkB-27AcK variants for both MgATP and F-6-P (Fig. 5C, D). Clearly, PfkA displayed cooperative kinetics with F-6-P and inhibition by MgATP, consistent with previous studies [8,51]. The PfkA-309AcK variant had similar patterns of saturation curves for both substrates, indicating that the acetylation at this site may not affect cooperative and inhibitive properties of PfkA. On the other hand, WT PfkB only showed inhibition by MgATP but no cooperativity with F-6-P, in alignment with previous studies [8,10,52]. The PfkB-27AcK variant had significantly decreased activities in both curves, consisting with recent studies that have demonstrated its essential role in both the catalysis and regulation of PfkB [53,54].

To exclude the possibility that the impaired activity results from non-specific effects such as misfolding or overall structure changes caused by lysine acetylation, we performed circular dichroism (CD) analysis of PfkA-309AcK and PfkB-27AcK variants. The CD spectra of both variants were similar to those of corresponding WT enzymes, indicating that lysine acetylation does not affect the overall structures of Pfk isozymes, and the decreased activity should be caused by specific effects of lysine acetylation on Pfk isozymes (Fig. 5E,F).

Regulation of Pfk isozymes by lysine acetylation in *E. coli* cells

Our *in vitro* enzyme assays for site-specific effects of lysine acetylation on Pfk isozymes were based on fully acetylated Pfk variants. However, the stoichiometry of acetylation at specific sites in living cells cannot reach 100% and is usually relatively low [35,36,55]. Thus, the impact of lysine acetylation on Pfk isozymes in cells may not be aligned well with the *in vitro* results. From the above experiments on acetylation and deacetylation processes of Pfk isozymes, we noted that native Pfk isozymes from various gene knockout strains had different lysine acetylation levels, which was ideal for evaluating the impact of lysine acetylation on Pfk isozymes in cells.

We first measured the enzyme activity of native PfkA purified from Δ*pfkB* and Δ*pfkB* Δ*ackA*, as well as native PfkB purified from Δ*pfkA* and Δ*pfkA* Δ*ackA* strains of *E. coli* BW25113 cells grown in 0.2% glucose media (Fig. 6). Although inactivation of *ackA* increased acetylation levels of both PfkA and PfkB (Fig. 4B), only the PfkB activity was affected

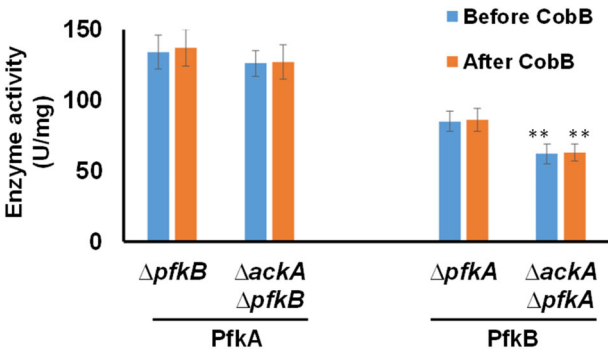

Fig. 6. The effects of lysine acetylation on Pfk isozymes in cells. Enzyme activities of native PfkA purified from Δ*pfkB* and Δ*pfkB* Δ*ackA* and native PfkB purified from Δ*pfkA* and Δ*pfkA* Δ*ackA* strains of *Escherichia coli* BW25113 cells grown in 0.2% glucose media before and after 1 h of CobB treatment. One unit (U) is defined as 1 μmol of product generation every 1 min. To measure the enzyme activity, both fructose 6-phosphate (F-6-P) and MgATP were fixed at 1 mM. The mean ± SD values were calculated based on three replicates. Two-tailed *P* values were determined via a *t*-test, and the significance level is 0.05. $^{**}P < 0.001$.

significantly. Our site-specific results showed that the fully acetylated PfkA variant at K309 retained approximately 70% of the WT PfkA activity and acetylation at other sites of PfkA had no significant effects (Fig. 5A). The activity of PfkA purified from the Δ*ackA* Δ*pfkB* strain was approximately 90% of that purified from the Δ*pfkB* strain, indicating that PfkA is only partially acetylated at K309 with accumulated AcP in cells. As for PfkB, full acetylation of PfkB K27 almost inactivated PfkB completely, whereas acetylation at other sites of PfkB had no significant effects (Fig. 5A). The activity of PfkB purified from the Δ*ackA* Δ*pfkA* strain was approximately 75% of that purified from the Δ*pfkA* strain, which also suggested PfkB is partially acetylated at K27 with an increased amount of AcP in cells.

Because CobB could deacetylate most of acetylated lysine residues in both Pfk isozymes, we further incubated above purified native Pfk isozymes with purified CobB and NAD^+ *in vitro*, and then measured their activities (Fig. 6). CobB-treatment could not restore Pfk isozyme activities, further indicating that K309 of PfkA and K27 of PfkB are resistant to CobB and these two sites are the major regulatory sites of lysine acetylation for Pfk isozymes.

Discussion

PfkA is a homotetramer and shows positive cooperativity with the substrate F-6-P, allosteric activation by ADP and GDP, and allosteric inhibition by PEP

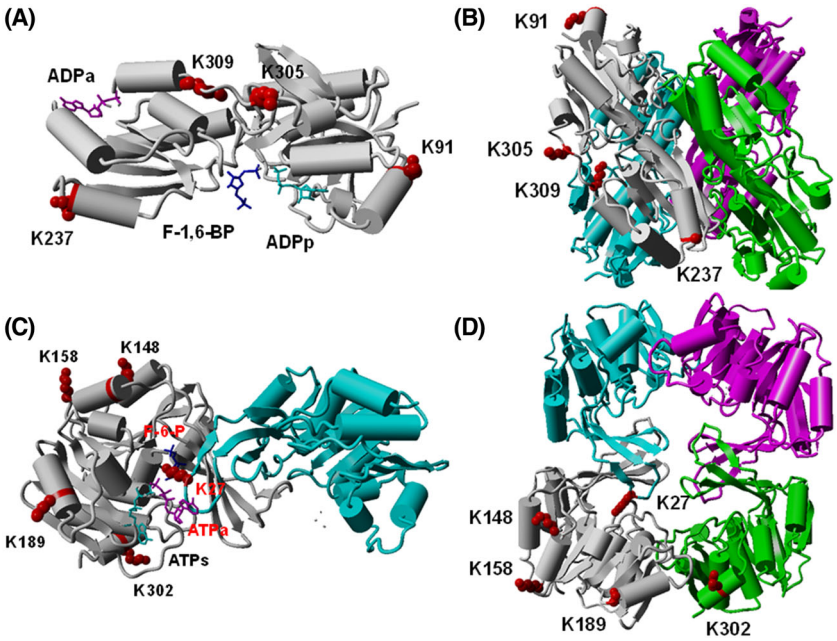

Fig. 7. Mapping of acetylation sites on the crystal structures of Pfk isozymes. (A) The monomer of PfkA (PDB ID: 1PFK). Acetylation sites are indicated in red. The product fructose 1,6-biphosphate (F-1,6-BP) is indicated in blue, the other product ADPp is indicated in cyan and the allosteric activator ADPa is indicated in purple. (B) The tetramer of PfkA (PDB ID: 1PFK). Four subunits are indicated in gray, purple, green and cyan. Acetylation sites are indicated in red. (C) The homodimer of PfkB (PDB ID: 3UQD). Acetylation sites are indicated in red. The substrate fructose 6-phosphate (F-6-P) is indicated in blue, the other substrate ATPs is indicated in cyan and the allosteric ATPa is indicated in purple. (D) The tetramer of PfkB (PDB ID: 3UQD). Four subunits are indicated in gray, purple, green and cyan. Acetylation sites are indicated in red. Structures were demonstrated using YASARA.

[8,51,56,57]. As for inhibition by the other substate, MgATP, there have been several mechanisms proposed, including substrate antagonism coupled with a steady-state random mechanism [58], the displacement of a pre-existing R-T equilibrium through an allosteric site for MgATP [59] and the allosteric communication between the active sites of different subunits [60]. We mapped the four acetylation sites on the crystal structure of PfkA (Fig. 7A,B) [56]. None of them are located at active sites, allosteric sites and interfaces between subunits. K91, K237 and K305 face outside to be accessible for CobB deacetylation, whereas K309 faces inside and resists CobB deacetylation. Although K309 of PfkA is not located at the active site, it faces the backbone of the active site. Replacement of K309 with glutamine or arginine did not affect enzyme activity (Fig. 5B), whereas acetylated K309, which has a bigger size than Lys, Gln or Arg, decreased PfkA activity. Thus, we proposed that acetylation of K309 could generate steric hindrance and shift the active site backbone to affect catalysis. This needs further structural analysis because the CD spectra of PfkA-309AcK did not show significant overall structural changes (Fig. 5E).

By contrast to PfkA, PfkB does not show cooperativity with the substrate F-6-P, allosteric activation by ADP and GDP, or allosteric inhibition by PEP [8]. However, both PfkA and PfkB are inhibited by MgATP, thus avoiding substrate F-6-P cycling and futile consumption of ATP [11]. PfkB is a homodimer and MgATP inhibition involves a dimer-to-tetramer transition [61]. We mapped the five acetylation sites on the crystal structure of PfkB (Fig. 7C,D) [54]. K148, K158, K189 and K302 face outside to be accessible for CobB deacetylation, whereas K27 faces inside and resists CobB deacetylation. K27 is located at the active site and interact with the substrate F-6-P and the allosteric MgATP. It has been proposed to prevent the simultaneous binding of F-6-P and allosteric MgATP and decrease the apparent affinity for substrate F-6-P by MgATP inhibition [53]. K27 has also been shown to stabilize the transition state of the dissociative mechanism [54]. The acetylation of K27 decreased the PfkB activity by almost 100-fold (Fig. 5A). The replacement of K27 by glutamine did not restore the activity, whereas the substitution of K27 with arginine restored a partial activity (Fig. 5B), indicating the essential role of the positive charge in catalysis. The

C-terminus of PfkB was shown to be important for MgATP-induced dimer-to-tetramer transition [50]. K302 is located at the C-terminal helix. The acetylation of K302 did not affect the enzyme activity. We mapped it onto the structure of the C-terminus of PfkB (Fig. S25). It faces to the different direction of I303, L307 and Y306 (essential residues for ternary and quaternary packing) [50], and so K302 may not affect the tetramerization induced by MgATP. The last residue of PfkB also faces to the different direction of those three key residues. This may explain why C-terminal His6-tag did not affect the enzyme activity as well as the saturation curves (Fig. S24).

Although we concluded that acetylation of K309 in PfkA and K27 in PfkB could affect the Pfk activity significantly based on testing fully acetylated Pfk variants generated by the genetic code expansion strategy, lysine acetylation only impacts PfkB function significantly in living *E. coli* cells because the stoichiometry of acetylation cannot reach 100% at one specific site in cells. A recent study also showed that incubation of PfkA with AcP *in vitro* could not affect its activity because of the relatively low stoichiometry of acetylation [46], which is consistent with our *in vivo* study with AcP-accumulated Δ*ackA* strains (Fig. 6). These studies demonstrate that it is necessary to consider the stoichiometry of acetylation in cells when determining the effect of acetylation on proteins. It is also noteworthy that those two regulatory sites, K309 of PfkA and K27 of PfkB, are also resistant to CobB deacetylase, implying that the impact of acetylation on Pfk isozymes will be accumulated and could not be reverted in cells.

Human cells also have two Pfk isozymes, PFK-1 and PFK2 [62]. Different from *E. coli* Pfk isozymes, only human PFK-1 can catalyze the production of F-1,6-BP from F-6-P. Human PFK-2 is a bifunctional enzyme that possesses both kinase (PFK-2) and phosphatase (FBPase-2) activities, catalyzing the generation and degradation of F-2,6-BP, which is a potent allosteric activator of PFK-1 [63]. Human PFK-1 has three isoforms, PFK-M (muscle), PFK-L (liver) and PFK-P (platelet), depending on the major tissues for expression [64], whereas PFK-2 has four isoforms, PFKFB1, PFKFB2, PFKFB3 and PFKFB4 [65]. Comparing the sequences of human and *E. coli* Pfk isozymes, all three human PFK-1 isoforms have more than 35% sequence identities with *E. coli* PfkA, showing a high homology between them. Several recent studies have shown that acetylation of animal PFK-1 can regulate its activity [66,67], indicating that acetylation of human PFK-1 could also have regulatory functions. However, we searched the lysine acetylation sites of human PFK-1 deposited to the acetylome database [25] and found no homologs of PfkA K309 in any of PFK-1 isoforms, indicating that the regulatory mechanism of acetylation on Pfk could be different between *E. coli* and human cells.

Materials and methods

Constructs and strains

DH5α cells (New England Biolabs, Ipswich, MA, USA) were used for gene cloning. Plasmids were constructed by the NEBuilder HiFi DNA Assembly Kit (New England Biolabs). Point mutations of the *pfkA* and *pfkB* genes in plasmids were introduced by the Q5 Site-Directed Mutagenesis Kit (New England Biolabs) and confirmed by whole-plasmid sequencing (Plasmidsaurus, Eugene, OR, USA). Gene knockout strains were obtained from the Keio collection in the laboratory inventory or constructed by homologous recombination [68]. The strains and plasmids used in the present study are listed in Table S1.

Recombinant expression of Pfk isozymes and variants

The genes of PfkA, PfkB and corresponding variants were inserted into the *pCDF-1b* plasmid and co-transformed into BL21 (DE3) cells (New England Biolabs) with the *pTech* plasmid containing the optimized AcK incorporation system. Cells were grown with 400 mL of LB medium (100 $\mu g \cdot mL^{-1}$ streptomycin and 50 $\mu g \cdot mL^{-1}$ chloramphenicol) at 37 °C until A_{600} of 0.8 was reached. Then, the expression of target proteins was induced by adding 0.2 mM isopropyl thio-β-D-galactoside. For AcK incorporation, growth media were supplemented with 10 mM AcK and 20 mM nicotinamine (the deacetylase inhibitor). Then, cells were further incubated with shaking at 16 °C for 12 h and harvested by centrifugation at 3000 ***g*** for 20 min at 4 °C. Collected cells were frozen and stored at −80 °C.

Purification of Pfk isozymes and variants

Frozen cells were resuspended in 10 mL of lysis buffer, which contains 50 mM Tris-HCl (pH 7.5), 300 mM NaCl, 20 mM imidazole, 5 mM β-mercaptoethanol, cocktail protease inhibitors and benzonase nuclease. Cells were then broken by sonication. Cell lysates were centrifuged at 20 000 ***g*** for 25 min at 4 °C. The supernatant was filtered by a 0.45-μm membrane and loaded to an Econo-Pac chromatography column (Bio-Rad, Hercules, CA, USA) with 2 mL of nickel-nitrilotriacetic acid resin equilibrated with 20 mL lysis buffer. The column was then washed with 20 mL of washing buffer, which contains 50 mM Tris-HCl (pH 7.5), 300 mM NaCl and 50 mM imidazole. The Pfk isozymes was eluted with 5 mL of elution buffer, which contains 50 mM Tris-HCl (pH 7.5), 300 mM NaCl and 200 mM imidazole. Purification of native PfkA and PfkB from

E. coli cells were implemented by following previous protocols [8,12].

General protein analyses

Protein concentrations were determined by the Bradford protein assay (Bio-Rad). Purified Pfk isozymes and their variants were loaded on 4–20% SDS/PAGE gels and stained by the Coomassie stain. Unstained SDS/PAGE gels were transferred onto poly(vinylidene difluoride) (PVDF) membranes using the Trans-Blot Turbo Transfer System (Bio-Rad). After transfer, PVDF membranes were shaken at room temperature with the blocking buffer (5% bovine serum albumin, 0.1% Tween 20 in Tris-buffered saline) for 2 h. After blocking, PVDF membranes were incubated with 1 : 1000 diluted horseradish peroxidase-conjugated acetyllysine antibody (Cell Signaling Technology, Danvers, MA, USA) overnight at 4 °C. Finally, PVDF membranes were visualized by chemiluminescence detection with the Pierce ECL western blotting kit (Thermo Fisher Scientific, Waltham, MA, USA).

MS analyses

The LC-MS/MS analyses were performed to determine lysine acetylation sites by following previous protocols [30]. Briefly, purified acetylated Pfk variants were fractionated by SDS/PAGE and stained. Corresponding gel bands were cut, digested by trypsin and analyzed using a LTQ Orbitrap XL mass spectrometer (Thermo Fisher Scientific) equipped with a nanoACQUITY UPLC system (Waters Corp., Milford, MA, USA). The Mascot search algorithm (https://www.matrixscience.com/server.html) was used to identify lysine acetylation sites.

The *in vitro* deacetylation and acetylation assays

The *in vitro* deacetylation assay was implemented in a total volume of 100 µL of 50 mM Hepes (pH 7.0), 5 mM $MgCl_2$, 1.0 mM NAD^+ and 1 mM dithiothreitol. Five micrograms of site-specifically acetylated Pfk isozyme variant was incubated with 2 µg of purified CobB at 37 °C for 1 h. The *in vitro* acetylation assay was performed in a total volume of 100 µL of 50 mM Hepes (pH 7.0), 0.1 mM EDTA, 1 mM dithiothreitol and 10 mM sodium butyrate. For YfiQ-dependent acetylation, 5 µg of purified WT PfkA or PfkB was incubated with 5 µg of purified YfiQ and 0.2 mM AcCoA at 37 °C for 1 h. For AcP-mediated chemical acetylation, 5 µg of purified WT PfkA or PfkB was incubated with 1 mM AcP at 37 °C for 1 h.

The Pfk enzyme activity assay

The initial velocity of phosphofructokinase activity was determined spectrophotometrically by coupling the F-1,6-BP production to the oxidation of NADH with aldolase, triosephosphate isomerase and glycerol 3-phosphate dehydrogenase [8]. Enzyme assays were performed in 25 mM Tris-HCl buffer (pH 8.2) [50]. A constant excess of 5 mM $MgCl_2$ higher than the concentration of ATP was used to ensure that majority of ATP exists as MgATP and to maintain free Mg^{2+} close to 5 mM [52]. Specific concentrations of F-6-P and MgATP were used in accordance with previous kinetic studies [8,69]. When determining enzyme activity, both F-6-P and MgATP were fixed at 1 mM, corresponding to the concentration at which maximum activity is reached. When determining the saturation curve of MgATP, the concentration of F-6-P was fixed at 1 mM, and the concentration of MgATP was varied at 10 µM, 33 µM, 100 µM, 330 µM, 1 mM, 3 mM and 6 mM; When determining the saturation curve of F-6-P, the concentration of MgATP was fixed at 1 mM, and the concentration of F-6-P was varied at 10 µM, 33 µM, 100 µM, 330 µM, 0.5 mM, 1 mM and 1.5 mM. Enzyme assays were implemented in 96-well plates and read with a microplate reader (Synergy HT; Biotek, Winooski, VT, USA) at 25 °C. The mean ± SD were calculated based on three replicates.

CD analysis

The CD spectra were recorded on a J-1500 CD Spectrometer (JASCO Corporation, Tokyo, Japan). Purified proteins were diluted to a concentration of 0.1 $mg{\cdot}mL^{-1}$ in 5 mM Tris-HCl, pH 7.8, 0.1 M KCl, and scanned from 190 to 250 nm with a speed of 60 $nm{\cdot}min^{-1}$. Scanning was performed five times for each sample and the average was plotted.

Acknowledgements

This research was funded by the National Institutes of Health (R15GM140433 and P20GM139768) and Arkansas Biosciences Institute.

Conflicts of interest

The authors declare that they have no conflicts of interest.

Author contributions

CF and XL designed the experiments and wrote the manuscript. All authors performed experiments, analyzed data and edited the manuscript.

Peer review

The peer review history for this article is available at https://www.webofscience.com/api/gateway/wos/peer-review/10.1111/febs.70014.

Data availability statement

The data that support the findings of the present study are available in the Supporting Information accompanying this article.

References

1 Wegener G & Krause U (2002) Different modes of activating phosphofructokinase, a key regulatory enzyme of glycolysis, in working vertebrate muscle. *Biochem Soc Trans* **30**, 264–270.
2 Hellinga HW & Evans PR (1985) Nucleotide sequence and high-level expression of the major *Escherichia coli* phosphofructokinase. *Eur J Biochem* **149**, 363–373.
3 Poorman RA, Randolph A, Kemp RG & Heinrikson RL (1984) Evolution of phosphofructokinase – gene duplication and creation of new effector sites. *Nature* **309**, 467–469.
4 Ronimus RS & Morgan HW (2001) The biochemical properties and phylogenies of phosphofructokinases from extremophiles. *Extremophiles* **5**, 357–373.
5 Bork P, Sander C & Valencia A (1993) Convergent evolution of similar enzymatic function on different protein folds: the hexokinase, ribokinase, and galactokinase families of sugar kinases. *Protein Sci* **2**, 31–40.
6 Daldal F & Fraenkel DG (1981) Tn10 insertions in the pfkB region of *Escherichia coli*. *J Bacteriol* **147**, 935–943.
7 Nakahigashi K, Toya Y, Ishii N, Soga T, Hasegawa M, Watanabe H, Takai Y, Honma M, Mori H & Tomita M (2009) Systematic phenome analysis of *Escherichia coli* multiple-knockout mutants reveals hidden reactions in central carbon metabolism. *Mol Syst Biol* **5**, 306.
8 Babul J (1978) Phosphofructokinases from *Escherichia coli*. Purification and characterization of the nonallosteric isozyme. *J Biol Chem* **253**, 4350–4355.
9 Zheng RL & Kemp RG (1992) The mechanism of ATP inhibition of wild type and mutant phosphofructo-1-kinase from *Escherichia coli*. *J Biol Chem* **267**, 23640–23645.
10 Guixe V & Babul J (1985) Effect of ATP on phosphofructokinase-2 from *Escherichia coli*. A mutant enzyme altered in the allosteric site for MgATP. *J Biol Chem* **260**, 11001–11005.
11 Torres JC, Guixe V & Babul J (1997) A mutant phosphofructokinase produces a futile cycle during gluconeogenesis in *Escherichia coli*. *Biochem J* **327**(Pt 3), 675–684.
12 Blangy D, Buc H & Monod J (1968) Kinetics of the allosteric interactions of phosphofructokinase from *Escherichia coli*. *J Mol Biol* **31**, 13–35.
13 Wang Y, San KY & Bennett GN (2013) Improvement of NADPH bioavailability in *Escherichia coli* through the use of phosphofructokinase deficient strains. *Appl Microbiol Biotechnol* **97**, 6883–6893.
14 Xie X, Liang Y, Liu H, Liu Y, Xu Q, Zhang C & Chen N (2014) Modification of glycolysis and its effect on the production of L-threonine in *Escherichia coli*. *J Ind Microbiol Biotechnol* **41**, 1007–1015.
15 Xia T, Han Q, Costanzo WV, Zhu Y, Urbauer JL & Eiteman MA (2015) Accumulation of d-glucose from pentoses by metabolically engineered *Escherichia coli*. *Appl Environ Microbiol* **81**, 3387–3394.
16 Li Y, Xian H, Xu Y, Zhu Y, Sun Z, Wang Q & Qi Q (2021) Fine tuning the glycolytic flux ratio of EP-bifido pathway for mevalonate production by enhancing glucose-6-phosphate dehydrogenase (Zwf) and CRISPRi suppressing 6-phosphofructose kinase (PfkA) in *Escherichia coli*. *Microb Cell Fact* **20**, 32.
17 Wang K, Wang X, Luo H, Wang Y, Wang Y, Tu T, Qin X, Bai Y, Huang H, Yao B *et al.* (2022) Synergetic fermentation of glucose and glycerol for high-yield N-acetylglucosamine production in *Escherichia coli*. *Int J Mol Sci* **23**, 773.
18 Wang Y, Chen E, Wang Y, Sun X, Dong Q, Chen P, Zhang C, Yang J & Sun Y (2024) Biosynthesis of mannose from glucose via constructing phosphorylation-dephosphorylation reactions in *Escherichia coli*. *Enzyme Microb Technol* **177**, 110427.
19 Yang J, Wu Y, Lv X, Liu L, Li J, Du G & Liu Y (2024) Engineering redox cofactor balance for improved 5-methyltetrahydrofolate production in *Escherichia coli*. *J Agric Food Chem* **72**, 9974–9983.
20 Carabetta VJ & Cristea IM (2017) Regulation, function, and detection of protein acetylation in bacteria. *J Bacteriol* **199**, e00107-17.
21 Christensen DG, Baumgartner JT, Xie X, Jew KM, Basisty N, Schilling B, Kuhn ML & Wolfe AJ (2019) Mechanisms, detection, and relevance of protein acetylation in prokaryotes. *MBio* **10**, e02708–e02718.
22 Liu M, Guo L, Fu Y, Huo M, Qi Q & Zhao G (2021) Bacterial protein acetylation and its role in cellular physiology and metabolic regulation. *Biotechnol Adv* **53**, 107842.
23 Christensen DG, Xie X, Basisty N, Byrnes J, McSweeney S, Schilling B & Wolfe AJ (2019) Post-translational protein acetylation: an elegant mechanism for bacteria to dynamically regulate metabolic functions. *Front Microbiol* **10**, 1604.
24 Van Drisse CM & Escalante-Semerena JC (2019) Protein acetylation in bacteria. *Annu Rev Microbiol* **73**, 111–132.
25 Zhang W, Tan X, Lin S, Gou Y, Han C, Zhang C, Ning W, Wang C & Xue Y (2022) CPLM 4.0: an updated database with rich annotations for protein lysine modifications. *Nucleic Acids Res* **50**, D451–D459.
26 Weeks J, Strom AI, Widjaja V, Alexander S, Pucher DK & Sohl CD (2021) Evaluating mechanisms of

IDH1 regulation through site-specific acetylation mimics. *Biomolecules* **11**, 740.
27 Xu Y, Liu L, Nakamura A, Someya S, Miyakawa T & Tanokura M (2017) Studies on the regulatory mechanism of isocitrate dehydrogenase 2 using acetylation mimics. *Sci Rep* **7**, 9785.
28 Wang X & Hayes JJ (2008) Acetylation mimics within individual core histone tail domains indicate distinct roles in regulating the stability of higher-order chromatin structure. *Mol Cell Biol* **28**, 227–236.
29 Venkat S, Chen H, Stahman A, Hudson D, McGuire P, Gan Q & Fan C (2018) Characterizing lysine acetylation of isocitrate dehydrogenase in *Escherichia coli*. *J Mol Biol* **430**, 1901–1911.
30 Fatema N, Li X, Gan Q & Fan C (2024) Characterizing lysine acetylation of glucokinase. *Protein Sci* **33**, e4845.
31 Neumann H, Peak-Chew SY & Chin JW (2008) Genetically encoding N(epsilon)-acetyllysine in recombinant proteins. *Nat Chem Biol* **4**, 232–234.
32 Weinert BT, Iesmantavicius V, Wagner SA, Scholz C, Gummesson B, Beli P, Nystrom T & Choudhary C (2013) Acetyl-phosphate is a critical determinant of lysine acetylation in *E. coli*. *Mol Cell* **51**, 265–272.
33 Kuhn ML, Zemaitaitis B, Hu LI, Sahu A, Sorensen D, Minasov G, Lima BP, Scholle M, Mrksich M, Anderson WF *et al.* (2014) Structural, kinetic and proteomic characterization of acetyl phosphate-dependent bacterial protein acetylation. *PLoS One* **9**, e94816.
34 Schilling B, Christensen D, Davis R, Sahu AK, Hu LI, Walker-Peddakotla A, Sorensen DJ, Zemaitaitis B, Gibson BW & Wolfe AJ (2015) Protein acetylation dynamics in response to carbon overflow in *Escherichia coli*. *Mol Microbiol* **98**, 847–863.
35 Meyer JG, D'Souza AK, Sorensen DJ, Rardin MJ, Wolfe AJ, Gibson BW & Schilling B (2016) Quantification of lysine acetylation and succinylation stoichiometry in proteins using mass spectrometric data-independent acquisitions (SWATH). *J Am Soc Mass Spectrom* **27**, 1758–1771.
36 Weinert BT, Satpathy S, Hansen BK, Lyon D, Jensen LJ & Choudhary C (2017) Accurate quantification of site-specific acetylation stoichiometry reveals the impact of Sirtuin deacetylase CobB on the *E. coli* acetylome. *Mol Cell Proteomics* **16**, 759–769.
37 Venkat S, Gregory C, Meng K, Gan Q & Fan C (2017) A facile protocol to generate site-specifically acetylated proteins in *Escherichia coli*. *J Vis Exp* **130**, e57061.
38 Hosseini MS, Sanaat Z, Akbarzadeh MA, Vaez-Gharamaleki Y & Akbarzadeh M (2024) Histone deacetylase inhibitors for leukemia treatment: current status and future directions. *Eur J Med Res* **29**, 514.
39 Thapa R, Moglad E, Afzal M, Gupta G, Bhat AA, Hassan Almalki W, Kazmi I, Alzarea SI, Pant K, Singh TG *et al.* (2024) The role of sirtuin 1 in ageing and neurodegenerative disease: a molecular perspective. *Ageing Res Rev* **102**, 102545.
40 Starai VJ, Celic I, Cole RN, Boeke JD & Escalante-Semerena JC (2002) Sir2-dependent activation of acetyl-CoA synthetase by deacetylation of active lysine. *Science* **298**, 2390–2392.
41 Zhao K, Chai X & Marmorstein R (2004) Structure and substrate binding properties of cobB, a Sir2 homolog protein deacetylase from *Escherichia coli*. *J Mol Biol* **337**, 731–741.
42 Hentchel KL & Escalante-Semerena JC (2015) Acylation of biomolecules in prokaryotes: a widespread strategy for the control of biological function and metabolic stress. *Microbiol Mol Biol Rev* **79**, 321–346.
43 Starai VJ & Escalante-Semerena JC (2004) Identification of the protein acetyltransferase (pat) enzyme that acetylates acetyl-CoA synthetase in *Salmonella enterica*. *J Mol Biol* **340**, 1005–1012.
44 Christensen DG, Meyer JG, Baumgartner JT, D'Souza AK, Nelson WC, Payne SH, Kuhn ML, Schilling B & Wolfe AJ (2018) Identification of novel protein lysine acetyltransferases in *Escherichia coli*. *MBio* **9**, e01905–e01918.
45 Takamura Y & Nomura G (1988) Changes in the intracellular concentration of acetyl-CoA and malonyl-CoA in relation to the carbon and energy metabolism of *Escherichia coli* K12. *J Gen Microbiol* **134**, 2249–2253.
46 Schastnaya E, Doubleday PF, Maurer L & Sauer U (2023) Non-enzymatic acetylation inhibits glycolytic enzymes in *Escherichia coli*. *Cell Rep* **42**, 111950.
47 Venkat S, Gregory C, Sturges J, Gan Q & Fan C (2017) Studying the lysine acetylation of malate dehydrogenase. *J Mol Biol* **429**, 1396–1405.
48 Venkat S, Chen H, McGuire P, Stahman A, Gan Q & Fan C (2019) Characterizing lysine acetylation of *Escherichia coli* type II citrate synthase. *FEBS J* **286**, 2799–2808.
49 Araujo J, Ottinger S, Venkat S, Gan Q & Fan C (2022) Studying acetylation of aconitase isozymes by genetic code expansion. *Front Chem* **10**, 862483.
50 Baez M, Merino F, Astorga G & Babul J (2008) Uncoupling the MgATP-induced inhibition and aggregation of *Escherichia coli* phosphofructokinase-2 by C-terminal mutations. *FEBS Lett* **582**, 1907–1912.
51 Auzat I, Le Bras G & Garel JR (1994) The cooperativity and allosteric inhibition of *Escherichia coli* phosphofructokinase depend on the interaction between threonine-125 and ATP. *Proc Natl Acad Sci USA* **91**, 5242–5246.
52 Cabrera R, Baez M, Pereira HM, Caniuguir A, Garratt RC & Babul J (2011) The crystal complex of phosphofructokinase-2 of *Escherichia coli* with fructose-

6-phosphate: kinetic and structural analysis of the allosteric ATP inhibition. *J Biol Chem* **286**, 5774–5783.
53 Villalobos P, Soto F, Baez M & Babul J (2016) Regulatory network of the allosteric ATP inhibition of *E. coli* phosphofructokinase-2 studied by hybrid dimers. *Biochimie* **128–129**, 209–216.
54 Murillo-Lopez J, Zinovjev K, Pereira H, Caniuguir A, Garratt R, Babul J, Recabarren R, Alzate-Morales J, Caballero J, Tunon I *et al.* (2019) Studying the phosphoryl transfer mechanism of the *E. coli* phosphofructokinase-2: from X-ray structure to quantum mechanics/molecular mechanics simulations. *Chem Sci* **10**, 2882–2892.
55 Baeza J, Dowell JA, Smallegan MJ, Fan J, Amador-Noguez D, Khan Z & Denu JM (2014) Stoichiometry of site-specific lysine acetylation in an entire proteome. *J Biol Chem* **289**, 21326–21338.
56 Shirakihara Y & Evans PR (1988) Crystal structure of the complex of phosphofructokinase from *Escherichia coli* with its reaction products. *J Mol Biol* **204**, 973–994.
57 Berger SA & Evans PR (1990) Active-site mutants altering the cooperativity of *E. coli* phosphofructokinase. *Nature* **343**, 575–576.
58 Wang X & Kemp RG (2001) Reaction path of phosphofructo-1-kinase is altered by mutagenesis and alternative substrates. *Biochemistry* **40**, 3938–3942.
59 Berger SA & Evans PR (1992) Site-directed mutagenesis identifies catalytic residues in the active site of *Escherichia coli* phosphofructokinase. *Biochemistry* **31**, 9237–9242.
60 Johnson JL & Reinhart GD (1992) MgATP and fructose 6-phosphate interactions with phosphofructokinase from *Escherichia coli*. *Biochemistry* **31**, 11510–11518.
61 Guixe V & Babul J (1988) Influence of ligands on the aggregation of the normal and mutant forms of phosphofructokinase 2 of *Escherichia coli*. *Arch Biochem Biophys* **264**, 519–524.
62 Dunaway GA (1983) A review of animal phosphofructokinase isozymes with an emphasis on their physiological role. *Mol Cell Biochem* **52**, 75–91.
63 Okar DA, Manzano A, Navarro-Sabate A, Riera L, Bartrons R & Lange AJ (2001) PFK-2/FBPase-2: maker and breaker of the essential biofactor fructose-2,6-bisphosphate. *Trends Biochem Sci* **26**, 30–35.
64 Fernandes PM, Kinkead J, McNae I, Michels PAM & Walkinshaw MD (2020) Biochemical and transcript level differences between the three human phosphofructokinases show optimisation of each isoform for specific metabolic niches. *Biochem J* **477**, 4425–4441.
65 Ros S & Schulze A (2013) Balancing glycolytic flux: the role of 6-phosphofructo-2-kinase/fructose 2,6-bisphosphatases in cancer metabolism. *Cancer Metab* **1**, 8.
66 Ren C, Chen L, Bai Y, Hou C, Li X, Schroyen M & Zhang D (2024) Comparative effects of phosphorylation and acetylation on glycolysis and myofibrillar proteins degradation in postmortem muscle. *Int J Biol Macromol* **257**, 128567.
67 Gandhirajan A, Roychowdhury S, Kibler C, Cross E, Abraham S, Bellar A, Nagy LE, Scheraga RG & Vachharajani V (2022) SIRT2-PFKP interaction dysregulates phagocytosis in macrophages with acute ethanol-exposure. *Front Immunol* **13**, 1079962.
68 Datsenko KA & Wanner BL (2000) One-step inactivation of chromosomal genes in *Escherichia coli* K-12 using PCR products. *Proc Natl Acad Sci USA* **97**, 6640–6645.
69 Parducci RE, Cabrera R, Baez M & Guixe V (2006) Evidence for a catalytic Mg^{2+} ion and effect of phosphate on the activity of *Escherichia coli* phosphofructokinase-2: regulatory properties of a ribokinase family member. *Biochemistry* **45**, 9291–9299.

Supporting information

Additional supporting information may be found online in the Supporting Information section at the end of the article.

Fig. S1. The protein sequence alignment of *E. coli* PfkA and PfkB.
Fig. S2. The full image of western blotting of purified PfkA variants.
Fig. S3. The full image of western blotting of purified PfkB variants.
Fig. S4. LC-MS/MS analysis of PfkA-91AcK.
Fig. S5. LC-MS/MS analysis of PfkA-237AcK.
Fig. S6. LC-MS/MS analysis of PfkA-305AcK.
Fig. S7. LC-MS/MS analysis of PfkA-309AcK.
Fig. S8. LC-MS/MS analysis of PfkB-27AcK.
Fig. S9. LC-MS/MS analysis of PfkB-148AcK.
Fig. S10. LC-MS/MS analysis of PfkB-158AcK.
Fig. S11. LC-MS/MS analysis of PfkB-189AcK.
Fig. S12. LC-MS/MS analysis of PfkB-302AcK.
Fig. S13. The full imaging of western blotting of CobB-treated Pfk variants.
Fig. S14. The full imaging of western blotting of native Pfk from Δ*cobB* cells.
Fig. S15. The full imaging of western blotting of native Pfk from Δ*yifQ* strains.
Fig. S16. The full imaging of western blotting of YfiQ-treated Pfk isozymes.
Fig. S17. The full imaging of western blotting of AcP-treated Pfk isozymes.
Fig. S18. LC-MS/MS analysis of AcP-treated PfkA.
Fig. S19. LC-MS/MS analysis of AcP-treated PfkA.
Fig. S20. LC-MS/MS analysis of AcP-treated PfkA.

Fig. S21. LC-MS/MS analysis of AcP-treated PfkB.
Fig. S22. LC-MS/MS analysis of AcP-treated PfkB.
Fig. S23. The full imaging of western blotting of native Pfk from Δ*pta* or Δ*ack* strains.
Fig. S24. The saturation curves of PfkB enzyme activity for MgATP and F-6-P.
Fig. S25. The structure of the C-terminus of PfkB.
Table S1. The list of strains with plasmids used in the present study.